中國機械工程學刊第四十三卷第六期第 539~547 頁(民國一百一十一年)
Journal of the Chinese Society of Mechanical Engineers, Vol.43, No.5, pp.539~547 (2022)

On the Design of Hybrid Systems with Continuously Variable Units utilizing a Basic Path Graph

Hsien-Yu Kuo* and Tyng Liu**

Keywords: continuously variable transmission (CVT), hybrid system, powertrain design

ABSTRACT

In this paper, a graphical method called the basic path graph (BPG) is utilized to synthesize the structure of hybrid systems with continuously variable units (CVUs). The symbols for the mechanical units and the classification of systems according to their characteristics are specified. Among them, two features are related to a wider ratio coverage and higher torque capacity. The systems can be synthesized with the Y-pattern, single-Δ-pattern, and double-Δ-pattern in a BPG. The total numbers of possible combinations are calculated. To ensure the viability of the system, the required mechanical units and their positions are specified. A detailed design example is provided. The result of the analysis shows that the overall ratio coverage for the synthesized system is 2.7 times wider than its CVU. The CVU only transfers 74% to 92% of the input torque and power. Therefore, it can also help to increase the torque capacity of the system.

INTRODUCTION

The role of the transmissions in road vehicles is to match the torque and efficiency characteristics of the power source with various driving situations. To improve energy efficiency, modern hybrid vehicles usually have multiple power sources, such as internal combustion engines (ICEs), motors/generators (M/Gs), and flywheels (FWs). The powertrains of hybrid vehicles need to combine the kinetic energy provided by two or more power sources and enable them to operate in high efficiency regions. Therefore, the requirement for an ideal transmission system includes a wide ratio coverage and high torque capacity.

Continuously variable units (CVUs) can provide seamless ratio variation. Their efficiency, ratio coverage, and torque capacity have been proven sufficient for vehicles ranging from scooters to full-size sport-utility vehicles. If the CVU can be integrated into hybrid system, the power sources will be more capable of operating under optimum conditions. In the references (Brockbank et al., 2009; Bongermino et al.,2017; Ceraolo et al., 2004; Dugger et al., 1971; Diego-Ayala et al., 2008; Debal et al., 2010; Frank et al., 1975; Greenwood, 1986; Gomez et al., 2004; Götz et al., 2016; Hagin et al., 1979; Höhn et al., 1994; Hofman et al., 2005; Höhn et al., 2006; He et al., 2008; Hu et al., 2019; Kok, 1999; Kinigadner et al., 2018; Loscutoff, 1976; Oba et al., 2002; Osone et al., 2014; Schilke et al., 1984; Spijker, 1994; Sheu et al., 2006; Trivić, 2012; Van Der Graaf, 1987; Yanagisawa et al., 2010), the topological structures of 28 hybrid systems were studied.

Among them, seven systems (Bongermino et al., 2017; Hagin et al., 1979; He et al., 2008; Hu et al., 2019; Kok, 1999; Oba et al., 2002) have two power sources coupled together via a speed-coupler, such as a two degrees-of-freedom (2DOF) planetary gear set (PG). There are also seven different systems (Diego-Ayala et al., 2008; Frank et al., 1975; Gomez et al., 2004; Hagin et al., 1979; He et al., 2008; Kok, 1999) with their CVUs combined with 2DOF planetary gear sets. The combination forms a power-split device that reduces the torque load of the CVU. However, two systems (Götz et al., 2016; Spijker, 1994; Van Der Graaf, 1987) have simpler designs. A constant ratio transmission mechanism is parallel to the CVU. In different operation modes, the driving power can be transmitted through the constant ratio path with higher efficiency and torque capacity. Moreover, three systems (Höhn et al., 1994, 2006; Schilke et al., 1984; Spijker, 1994; Van Der Graaf, 1987) are able to have driving power flow through the CVUs in opposite directions under different operation modes. Therefore, the ratio coverages for the CVUs are exploited twice. The total ratio coverages for the systems are enlarged.

Generally, hybrid systems are categorized into three types, parallel, series, and power split, according to the coupling pattern of the power sources. To express the structure of the system in a more detailed way, Chen (2015) developed a graphical method called the function power graph (FPG). In the FPG, the transmission paths for the kinetic energy are shown with connection lines. Mechanical units are depicted by various symbols. To reduce the difficulties in analyzing existing systems and

Paper Received January, 2022. Revised October, 2022, Accepted December, 2022, Author for Correspondence: Hsien-Yu Kuo.

* *Ph.D. Candidate, Department of Mechanical Engineering, National Taiwan University, Taipei, Taiwan 10617, ROC.*

** *Associate Professor, Department of Mechanical Engineering, National Taiwan University, Taipei, Taiwan 10617, ROC.*

synthesizing other possible configurations, a simplified graphical method named the basic path graph (BPG) is proposed (Kuo, 2021) based on a FPG. In a BPG, only the key elements of the system are represented. All other units are ignored for better simplicity. Therefore, the researcher can better focus on the layout of the power transmission paths. This can help to develop a system with wider ratio coverage and higher torque capacity.

BASIC PATH GRAPH (BPG)

Basic Units

Eight different units are taken into account in a BPG, including power input, output, CVU, and multiple degrees of freedom units, as listed in Table 1. When synthesizing a new system, the undetermined unit is used to represent the unit or the topological structure that needs to be determined according to the requirement of the system.

Table 1. List of basic units

Unit	Symbol	Description
IN	IN	Power input such as ICE, M/G, and FW.
O	O	Power output, can be an individual wheel or driving axle including the differential.
CVU	CVU	Transmission mechanism with continuously variable ratio.
2DOF-3E	2dof	2DOF gear set with three basic elements, such as planetary gear set.
2DOF-4E	2dof	2DOF gear set with four basic elements, such as Ravigneaux gear set.
Connection line		Transmission path for kinetic energy.
Coupling point		Intersection of three or more connection lines.
U	U	Undetermined mechanism.

Classification of the systems

To describe the energy coupling pattern and the application of the CVU, the hybrid systems with CVUs can be sorted into 12 categories according to the following three characteristics (Kuo, 2021):

(1) Direction of power flows through the CVU: one-way or dual-way manipulated.
(2) Coupled pattern of the power inputs: torque-coupled or speed-coupled.
(3) Number of power transmission paths parallel to the CVU: mono-path, bypass-type dual-path, or power-split-type dual-path.

The first is related to the ability of the system to exploit the ratio coverage for the CVU. Most of the studied systems are one-way manipulated. The driving power flowing through the CVU is unidirectional. For a dual-way manipulated system, the input and output shafts of the CVU can be interchanged under different operation modes. Therefore, its ratio coverage is exploited twice. A bridge structure is required in the BPG for the system. The structure comprises three undetermined units, as depicted in Fig. 1(a). The undetermined units U_1 and U_3 can be a coupling point or a multi-DOF unit that can be connected to 3 or more connection lines. U_2 can be either a CVU or a more complicated structure comprising a CVU.

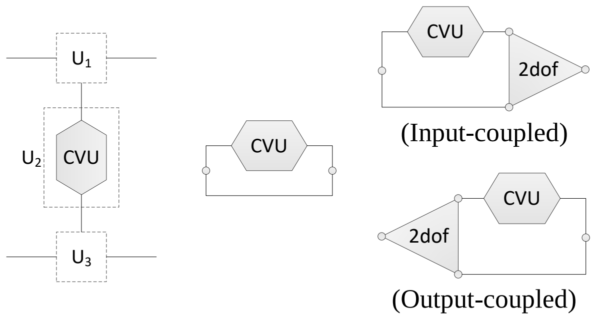

(a) Bridge (b) Bypass loop (c) Power-split loop

Fig. 1. Required structures for dual-way manipulated systems, bypass-type dual-path systems, and power-split-type dual-path systems in a BPG

The second characteristic is determined by whether the kinetic energy for different power inputs is merged on a multi DOF unit, also called a speed-coupler. For a torque-coupled system, the kinetic energy is merged on a coupling point. The torque distribution among the power inputs is arbitrary, while the rotational speed is the same. For a speed-coupled system, the speed ratio and the steady-state torque distribution are both constant and determined by the gear ratio of the multi-DOF unit.

The third characteristic is related to the torque capacity of the system. All of the input powers are transmitted solely by the CVU in a mono-path system. For a bypass-type dual-path system, there is a direct-drive path parallel to the CVU, as shown in Fig. 1(b). The power can be transmitted either by the CVU or the direct-drive path with a higher efficiency and torque capacity. However, in the CVU-driven mode, the torque capacity is still confined by the CVU. Power cannot be transferred by both types of transmission unless the ratios are exactly the same. For a power-split-type dual-path system, the CVU and the direct-drive path are combined with a multi DOF gear set, as shown in Fig. 1(c). The input power can be transmitted by the direct-drive path and the CVU simultaneously. Thus, the maximum allowable torque of the system can be increased.

SYSTEM SYNTHESIS WITH A BPG

With the aid of a BPG, the transmission paths for the kinetic energy within the system can be clearly displayed. When synthesizing the system, different basic units or structures are inserted into the undetermined units of the system. To form a hybrid system with a continuously variable ratio, one of the undetermined units must contain a CVU, bypass loop, or power-split loop. After selecting the desired layout from the synthesized results, other mechanical units can be added into the system, and the structure of the system in the FPG is completed.

Synthesis of the one-way manipulated system

Among the 28 studied systems, the BPGs for the most one-way manipulated systems belong to the Y-pattern, which is shown in Fig. 2. The pattern comprises four undetermined units. Only U_2 is connected to three connection lines, and the other three are connected to two connection lines. The content of the undetermined unit with two connection lines needs to be a basic unit or a combination of multiple basic units that can also be connected to two connection lines. Therefore, the possible contents are a connection line, a CVU, a bypass loop, or a power-split loop. For the undetermined unit with three connection lines, the content should be a basic unit that can be connected to three connection lines. The possible contents are a coupling point or a 2DOF-3E unit.

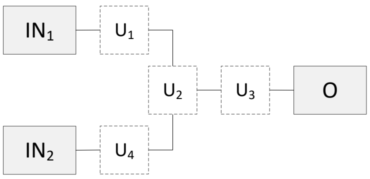

Fig. 2. Y-pattern in a BPG

If only one CVU is allowed to exist in the system, the content of the one unit among U_1, U_3, and U_4 can be a CVU, a bypass loop, or a power-split loop with two connecting patterns (input-coupled or output-coupled). There are four options in total. The other two undetermined units can only be connection lines. Meanwhile, the number of options for the content of U_2 is two. Therefore, the total number of possible combinations of the system can be calculated from equation (1).

$$(C_1^{(5-1)} \times C_1^3) \times C_1^2 = (4 \times 3) \times 2 = 24. \qquad (1)$$

Synthesis of the dual-way manipulated system

Only three dual-way manipulated systems have been reported in the literature (Höhn et al., 1994, 2006; Schilke et al., 1984; Spijker, 1994; Van Der Graaf, 1987). Among them, two systems (Höhn et al., 1994, 2006; Schilke et al., 1984) belong to the single-Δ-pattern shown in Fig. 3(a), whereas the other system (Spijker, 1994; Van Der Graaf, 1987) has the double-Δ-pattern shown in Fig. 3(b). The number of undetermined units in the single-Δ-pattern is four. U_1 to U_3 are connected to three connection lines, and U_4 is the only unit that is connected to two connection lines. The four units form a looped structure. U_4 is also located at the center of the bridge structure of the dual-way manipulated system. In the double-Δ-pattern, there are five undetermined units. U_2 to U_4 are connected to three connection lines, whereas U_1 is connected to four connection lines, and U_5 is connected to two connection lines. Two looped structures are formed by the connection lines in the double-Δ-pattern. U_5 is located at the center of the bridge structure.

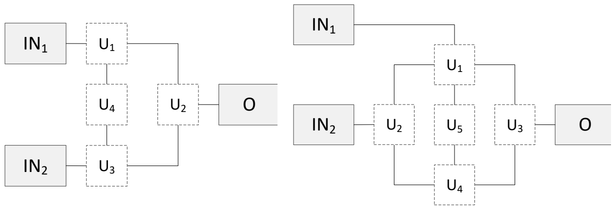

(a) Single-Δ-pattern (b) Double-Δ-pattern

Fig. 3. Single-Δ-pattern and double-Δ-pattern in a BPG

Similar to the Y-pattern, the content of the undetermined units that are connected to three connection lines can be either a coupling point or a 2DOF-3E unit. For a unit with four connection lines, the content can be either a coupling point or a 2DOF-4E unit. For the undetermined unit with two connection lines, the options for its content can be a CVU, a bypass loop, or a power-split loop with two connecting patterns.

In the single-Δ-pattern, the contents of the three undetermined units with three connection lines have two options. The content of the undetermined unit with two connection lines has four options. Therefore, the number of total possible combinations of the dual-way manipulated system with a single-Δ-pattern can be calculated from equation (2).

$$C_1^4 \times (C_1^2)^3 = 4 \times 2^3 = 32. \qquad (2)$$

In the double-Δ-pattern, the contents of the three undetermined units with three connection lines and the one unit with four connection lines also have 2 options. The content of the unit with two connection lines has four options. Therefore, the result can be calculated from equation (3).

$$C_1^4 \times (C_1^2)^3 \times C_1^2 = 4 \times 2^3 \times 2 = 64. \qquad (3)$$

Assessment of the viability of synthesized systems

When developing the complete FPG for the system based on its BPG, extra units, such as clutches and gear sets, must be added to the connection lines. To avoid the possibility that the synthesized mechanism is unable to achieve the desired feature or even if it is implausible, the viability of the result should be assessed. The five mechanisms shown in Table 2 are considered when assessing the viability of the system. Two of them are coaxial mechanisms, including a clutch and planetary gear set. The other three mechanisms have noncoaxial input and output axes, including a V-belt CVU, gear set, and chain drive.

Table 2. Configuration of input and output axes for units

and subsystems

	Coaxial		Noncoaxial		
Unit	Clutch	PG	CVU	Gear set	Chain drive
Symbol in FPG	C	c PG r s	CVU	G	Ch
Schematic	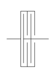	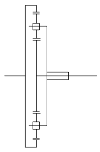	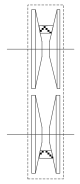	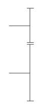	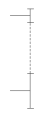

If the BPG comprises a looped structure with the CVU, such as a bypass loop or a power-split loop, at least a noncoaxial mechanism is required in the loop to connect the two shafts of the CVU. Furthermore, a shifting clutch (SC) or two independent clutches are required in the bypass loop to direct the power through one of the two paths. For the bridge structure of dual-way manipulated systems, four clutches are required to isolate the idling transmission path under different operation modes. Each clutch is located upstream and downstream of the two parallel paths of the bridge structure. Viable examples for a bypass loop, a power-split loop, and a bridge structure are provided in Fig. 4 to Figure Fig. 6.

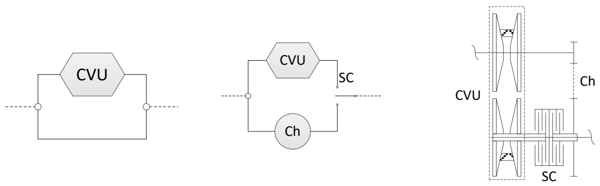

(a) BPG (b) FPG (c) Schematic

Fig. 4. Viable example of the bypass loop structure

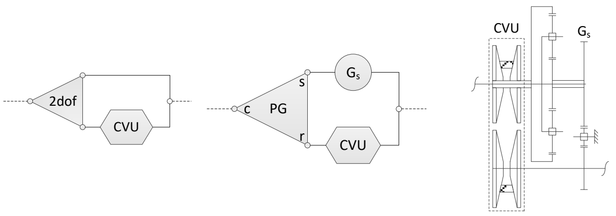

(a) BPG (b) FPG (c) Schematic

Fig. 5. Viable example of the power-split loop structure

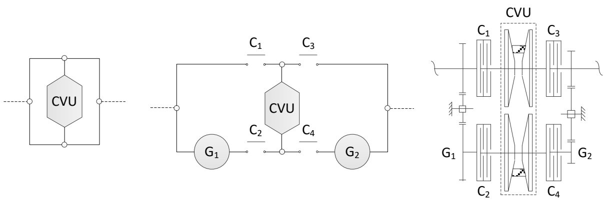

(a) BPG (b) FPG (c) Schematic

Fig. 6. Viable example of the bridge structure

DESIGN EXAMPLE

In this chapter, a dual-way manipulated system with a single-Δ-pattern is used as an example. The system can provide wider overall ratio coverage, and the layout is simpler than that for the system with the double-Δ-pattern. To realize a higher torque capacity and continuous ratio variation, the system should be power-split-type dual-pathed. The coupling pattern for different power inputs is chosen to be torque-coupled because the steady-state torque distribution between the two power inputs can be arbitrary. A simpler configuration with the above characteristics is depicted in Fig. 7(a) and is one of the 32 results obtained from equation (2).

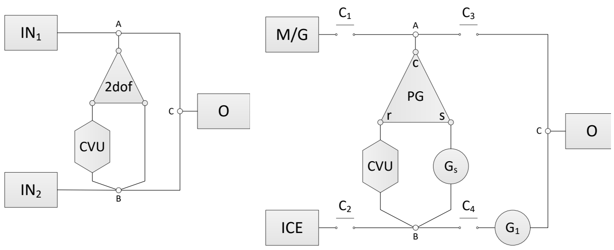

(a) BPG (b) FPG

Fig. 7. BPG and complete FPG for the system

According to the previous section, four clutches should be inserted up- and downstream of the bridge structure. There are two loops in the layout of the system; therefore, two noncoaxial gear sets G_s and G_1 are required in each loop. After determining the connecting pattern for the 2DOF-3E unit and the types of power inputs, the layout in the FPG is completed, as shown in Fig. 7(b).

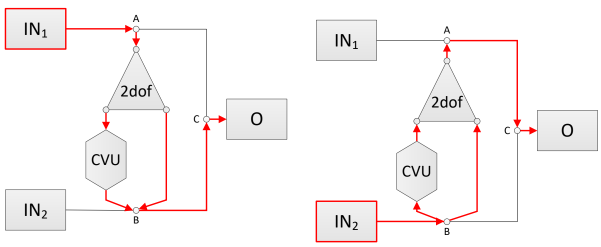

(a) Mode 1: $IN_1 \rightarrow O$ (b) Mode 2: $IN_2 \rightarrow O$

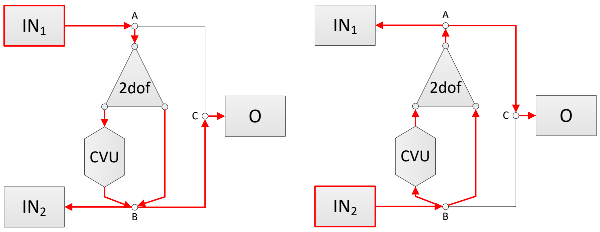

(c) Mode 3: $IN_1 \rightarrow IN_2$+O (d) Mode 4: $IN_2 \rightarrow IN_1$+O

Fig. 8. Power flow patterns with a single power source

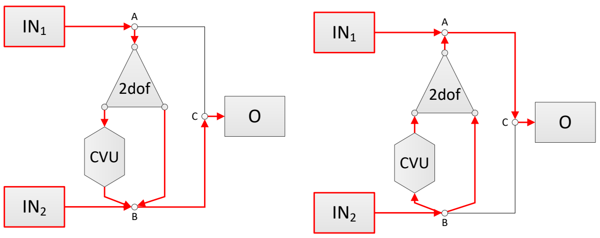

(a) Mode 5: IN_1+$IN_2 \rightarrow$O (b) Mode 6: IN_1+$IN_2 \rightarrow$O

Fig. 9. Power flow patterns with double power sources

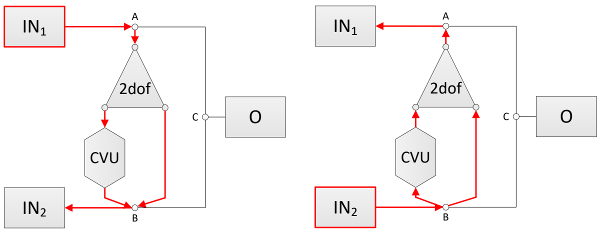

(a) Mode 7: $IN_1 \rightarrow IN_2$ (b) Mode 8: $IN_2 \rightarrow IN_1$

Fig. 10. Power flow patterns for neutral modes with internal power flow

The possible power flow patterns can then be formulated, as shown in Fig. 8 to Figure Fig. 10. Among them, only in modes 1 and 2 is the output purely driven by one of the inputs, while there no other unit receives energy. Therefore, as shown in Fig. 11, two modes can be used as the basic operation modes for the powertrain: the EV mode and engine mode.

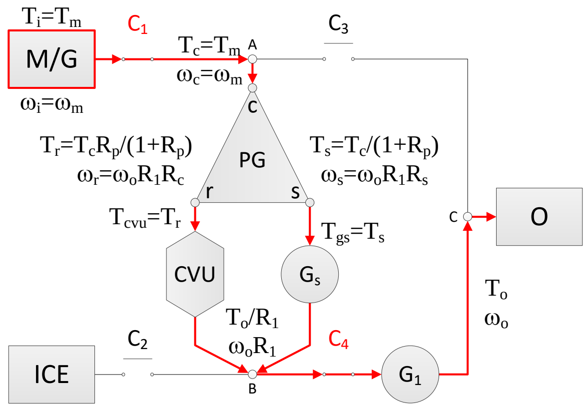

(a) EV mode

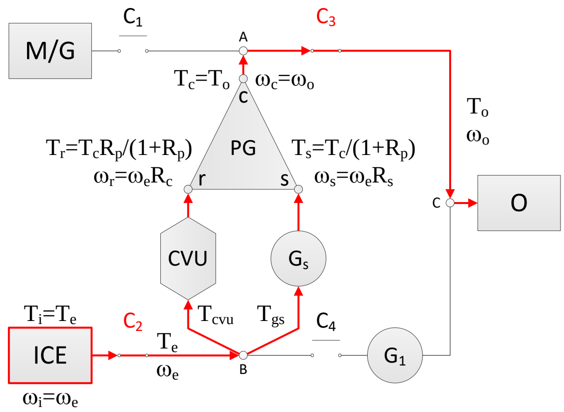

(b) Engine mode

Fig. 11. Torque, speed, and power flow pattern in the two basic operation modes

If the energy loss of the units is not considered, the kinematic model of the system can be derived. The system ratio $R_{sys.ev}$ in EV mode can be calculated with equation (4).

$$R_{sys.ev} = \frac{\omega_m}{\omega_o} = \frac{R_1 R_s + R_1 R_p R_c}{1 + R_p}. \quad (4)$$

The fraction of the torque and the power transferred by the CVU under EV mode, or the torque-split ratio $r_{ts.ev}$ and the power-split ratio $r_{ps.ev}$, can be expressed using equations (5) and (6). P_{cvu} stands for the power transferred by the CVU and P_{input} for the total input power of the system.

$$r_{ts.ev} = \frac{T_{cvu}}{T_i} = \frac{T_r}{T_m} = \frac{R_p}{1 + R_p}. \quad (5)$$

$$r_{ps.ev} = \frac{P_{CVU}}{P_{input}} = \frac{R_p R_c}{R_s + R_p R_c}. \quad (6)$$

In engine mode, the system ratio $R_{sys.ic}$ can be calculated using equation (7).

$$R_{sys.ic} = \frac{\omega_e}{\omega_o} = \frac{1 + R_p}{R_s + R_p R_c}. \quad (7)$$

The torque-split ratio $r_{ts.ic}$ and the power-split ratio $r_{ps.ic}$ for the system under engine mode can be expressed using equations (8) and (9). P_{output} stands for the total output power of the system. Because the power loss in the system is not considered, its value is equivalent to P_{input}.

$$r_{ts.ic} = \frac{T_{cvu}}{T_i} = \frac{T_{cvu}}{T_{cvu} + T_{gs}} = \frac{R_p R_c}{R_p R_c + R_s}. \quad (8)$$

$$r_{ps.ic} = \frac{P_{CVU}}{P_{output}} = \frac{R_p R_c}{R_s + R_p R_c}. \quad (9)$$

RESULTS

To provide continuous ratio variation during mode switching, the ratio coverages for EV mode and engine mode should join together or have a small overlap region. The possible combination of the parameters can be found by the global search method and is listed in Table 3. Because the ratios of the three gear sets are all rational numbers, the gears in the system are machinable. The layout for the mechanism can be arranged as shown by the schematic in Fig. 12 with the addition of an extra final drive gear set G_f.

Table 3. Values for the system parameters

Parameter	Value	Parameter	Value
R_p	2.857 (20/7)	$R_{c.Max}$	2.0
R_s	0.5	$R_{c.min}$	0.5
R_1	2.0		

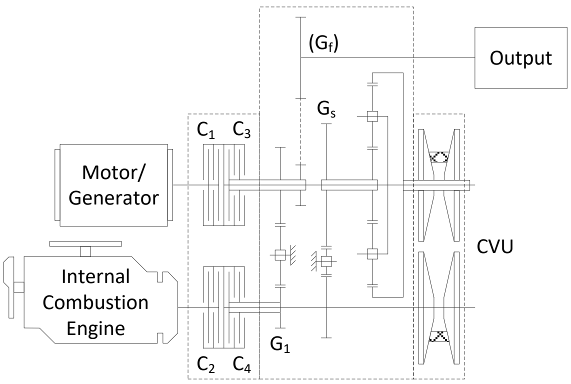

Fig. 12. Schematic of the system

With the aid of MATLAB, the variation in the system's ratio, the torque-split ratio, and the power-split ratio according to the CVU ratio can be analyzed. As shown in Fig. 13, the system ratio under EV and engine modes is shown. The overall ratio coverage of the system is 10.7 (=6.4/0.6), which is 2.7 times wider than the ratio span of the CVU (2.0/0.5=4.0). The system still possesses continuous ratio variation because the system ratio remains at 2.0 during mode switching.

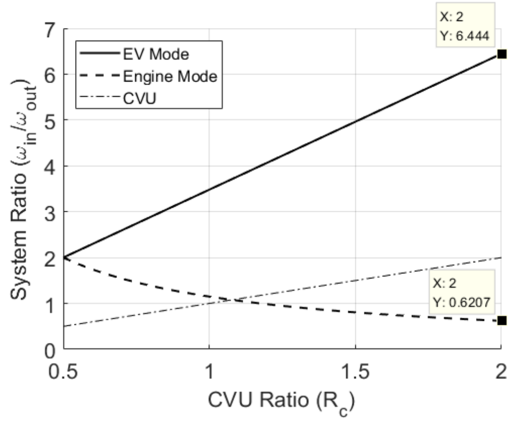

Fig. 13. System ratio in both modes compared with the CVU

The variation in the torque-split ratio and the power-split ratio is shown in Figure 14 and Figure 15. As shown in Fig. 14, the torque-split ratio remains constant under EV mode regardless of the variation in the system ratio. This means that only 74% of the input torque is transferred by the CVU in EV mode. When the vehicle is in engine mode, the transferred torque for the CVU rises while the system ratio approaches the maximum overdrive. The fraction of the transferred torque for the CVU reaches a maximum value of 92% when the system ratio is at a minimum value of 0.62. As shown in Fig. 15, the variation in the power-split ratio under both modes follows the same curve, so the fraction of the power transmitted by the CVU varies from 74% to 92% according to the CVU's ratio. Thus, the system can reduce the transferred torque and power for the CVU, especially during situations with higher torque loading, such as hill climbing and accelerating from a standstill.

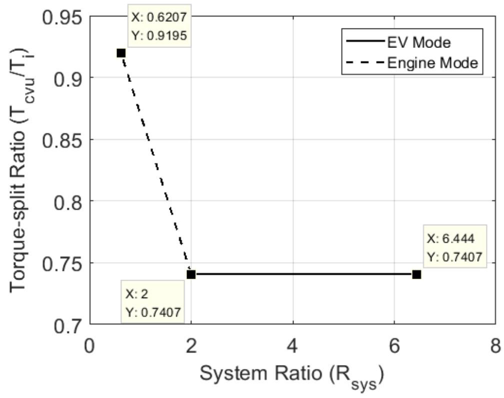

Fig. 14. Variation in the torque-split ratio

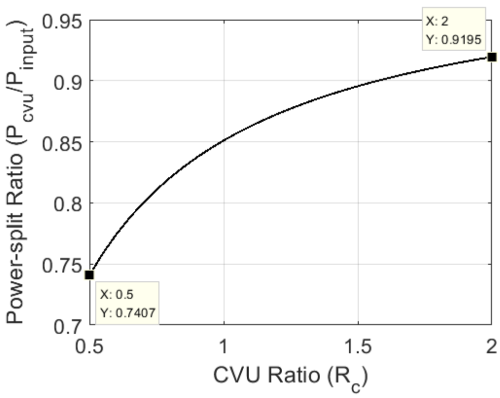

Fig. 15. Variation in the power-split ratio

CONCLUSIONS

In this paper, the process of synthesizing a hybrid system that comprises a CVU is proposed. First, the BPG and its elements are introduced. The three characteristics of hybrid systems with CVUs and their requirements are explained.

By analyzing the topological structures of the 28 existing systems, their BPGs can be sorted into three patterns: Y-pattern for one-way manipulated systems, single-Δ-pattern and double-Δ-pattern for dual-way manipulated systems. The system can be synthesized based on the three patterns. The total numbers of possible configurations can be calculated. There are 24 types of one-way manipulated systems, 32 dual-way manipulated systems with single-Δ-patterns, and 64 dual-way manipulated systems with double-Δ-patterns.

To ensure that the developed mechanism can exist in reality, the viability of the system should be assessed. A noncoaxial transmission mechanism is required in the looped structure to connect the two shafts of the V-belt CVU. In the bypass loop, the clutch arrangement should allow the energy to be transferred either through the CVU or the direct-drive path. For the bridge structure of the dual-way manipulated systems, four clutches should be located upstream and downstream of the bridge structure.

Furthermore, a detailed design with a single-Δ-pattern is provided. A complete topological structure is developed, and the kinematic model is established. The variations in the system ratio, torque-split ratio, and power-split ratio under EV mode and engine mode are analyzed. The result shows that the system's overall ratio coverage is 2.7 times wider than that of the CVU. The CVU only transfers 74% to 92% of the input torque and power. Therefore, the synthesized system has a larger overall ratio coverage and increased torque capacity.

ACKNOWLEDGMENT

This study has been supported by Giant Lion Know-How Co., Ltd., which is gratefully acknowledged by the authors.

REFERENCES

Brockbank, C., and Greenwood, C., "Full-toroidal variable drive transmission systems in mechanical hybrid systems–from Formula 1 to road vehicles," CTI Symposium and Exhibition: Automotive Transmissions, Detroit, MI (2009).

Bongermino, E., Tomaselli, M., Monopoli, V. G., Rizzello, G., Cupertino, F., and Naso, D., "Hybrid aeronautical propulsion: control and energy management," *IFAC-PapersOnLine*, Vol. 50(2), pp. 169–174 (2017).

Ceraolo, M., Caleo, A., Capozzella, P., Marcacci, M., and Carmignani, L., "Operation and performance of a small scooter with a parallel-hybrid drive-train," *SAE Paper* No. 2004-32-0077 (2004).

Chen, I.M., Yang, T.H., and Liu, T., "Function Power Graph—A novel methodology for powertrain and hybrid system conceptual design and analysis," Proc., of the 2015 IFToMM World Congress, Taipei, Taiwan (2015).

Dugger, G., Brandt A., George, J., and Perini, L., "Flywheel and flywheel/heat engine hybrid propulsion systems for low-emission vehicles," Proc., of Intersociety Energy Conversion Engineering Conference, Boston, MA (1971).

Diego-Ayala, U., Martinez-Gonzalez, P., and McGlashan, N., "The mechanical hybrid vehicle: An investigation of a flywheel-based vehicular regenerative energy capture system," *Proc. I. Mech. E., Part D: J. of Automobile Engineering*, Vol. 222(11), pp. 2087–2101 (2008).

Debal, P., Faid, S., Tricoche, L., and Bervoets, S., "CVT-based full hybrid powertrain offering high efficiency at lower cost," *SAE Paper* No. 2010-01-1313 (2010).

Frank, A.A., and Beachley, N., "Improved fuel economy in automobiles by use of a flywheel energy management system," Proc., of the 1975 Flywheel Technology Symposium, Berkeley, CA (1975).

Greenwood, C.J., "Integration of a commercial vehicle regenerative braking driveline," *I. Mech. E.*, C191/86, pp. 127-133 (1986).

Gomez, M., Mucino, V., Clark, N., and Smith, J., "A configuration for a continuously variable power-split transmission in hybrid-electric vehicle applications," *SAE Paper* No. 2004-01-0571 (2004).

Götz, A., Lauinger, C., Walter, B., and Finsterbusch, M., "Efficient CVT for plug-in hybrid vehicles," *ATZ Worldwide*, Vol. 118(12), pp. 26–31 (2016).

Hagin, F., and Merker, P., "Drive systems with brake-energy recovery," Proc., of the First International Automotive Fuel Economy Research Conference, Washington D.C. (1979).

Höhn, B.R., and Pinnekamp, B., "The Autarc Hybrid: A universal power train concept for passenger cars," *ATZ-Automobiltechnische Zeitschrift*, Vol. 96(5), pp. 294-300 (1994).

Hofman, T., Van Druten, R., Serrarens, A., and Van Baalen, J., “A fundamental case study on the Prius and IMA drivetrain concepts,” Proc. of the 21st International Battery, Hybrid and Fuel Cell Electric Vehicle Symposium & Exposition, Monaco (2005).

Höhn, B.R., Pflaum, H., and Tomic, D., “Fuel consumption and energy balance of ‘Optimized CVT-hybrid-driveline’,” *SAE Paper* No. 2006-01-3259 (2006).

He, L., Wu, G., Meng, X., and Sun, X., “A novel continuously variable transmission flywheel hybrid electric powertrain,” Proc. of the IEEE Vehicle Power and Propulsion Conference, Harbin, China (2008).

Hu, J., Mei, B., Peng, H., and Jiang, X., “Optimization design and analysis for a single motor hybrid powertrain configuration with dual planetary gears,” *Appl. Sci.*, Vol. 9(4): 707 (2019).

Kok, D.B., *Design optimization of a flywheel hybrid vehicle*, Ph. D. Thesis, Eindhoven University of Technology, Eindhoven, The Netherlands (1999).

Kinigadner, A., Lauinger, C., and Vornehm, M., “Dedicated hybrid transmission,” http://schaeffler-events.com/symposium/lecture/h6/index.html (2018, accessed on 2 December 2021).

Kuo, H.Y., and Liu, T., “On the design of continuously variable transmissions with bidirectional bridge structures for hybrid vehicles,” *Appl. Sci.*, Vol. 11(6): 2500 (2021).

Loscutoff, W.V., *Flywheel/Heat engine power for an energy-economic personal vehicle*, BNWL-2006, Battelle Pacific Northwest Labs., Richland, WA (1976).

Oba, H., Yamanaka, A., Katsuta, H., and Kamichi, K., “Development of a hybrid powertrain system using CVT in a minivan,” *SAE Paper* No. 2002-01-0991 (2002).

Osone, T., Seiji, T., Yamamoto, T., and Konagaya, F., “Development of Jatco CVT8 hybrid for Infiniti JX and Nissan Pathfinder,” *SAE Paper* No. 2014-01-1788 (2014).

Schilke, N. A., DeHart, A. O., Hewko, L. O., Matthews, C. C., Pozniak, D. J., and Rohde, S. M., “The design of an engine-flywheel hybrid drive system for a passenger car,” *SAE Transactions*, Vol. 93, pp. 779-799 (1984).

Spijker, E., *Steering and control of a CVT based hybrid transmission for a passenger car*, Ph. D. Thesis, Eindhoven University of Technology, Eindhoven, The Netherlands (1994).

Sheu, K.B., Hsu, T.H., and Hsu, Y.Y., “A novel parallel hybrid motorcycle transmission,” *J. of Mater. Sci. Forum*, Vol. 505-507, pp. 1021–1026 (2006).

Trivić, I., *Comparative analysis of alternative hybrid systems for automotive applications*, Ph. D. Thesis, University of Bologna, Bologna, Italy (2012).

Van Der Graaf, R., “An IC engine-flywheel hybrid drive for road vehicles,” Proc., of the International Conference on New Developments in Power Train and Chassis Engineering, Strasbourg, France (1987).

Yanagisawa, T., Yamanishi, T., Utsugi, K., and Nagatsuyu, T., “Development of idling stop system for 125 cm3 scooters with fuel injection,” *SAE Paper* No. 2010-32-0121 (2010).

NOMENCLATURE

P_{input}	Input power
P_{output}	Output power
P_{CVU}	Power transferred by the CVU
R_c	Ratio of the CVU
R_p	Ratio of the planetary gear set PG
R_s	Ratio of the gear set G_s
R_1	Ratio of the gear set G_1
R_{sys}	System Ratio
r_{ts}	Torque-split ratio
r_{ps}	Power-split ratio
ω_i	Input speed of the system
ω_o	Output speed of the system
ω_m	Rotational speed of M/G
ω_e	Rotational speed of ICE
ω_c	Rotational speed of the carrier
ω_r	Rotational speed of the ring gear
ω_s	Rotational speed of the sun gear
T_i	Input torque of the system
T_o	Output torque of the system
T_m	Input torque from M/G
T_e	Input torque from ICE
T_{cvu}	Input torque of the CVU
T_{gs}	Input torque of the gear set G_s
T_c	Torque exerted on the carrier
T_r	Torque exerted on the ring gear
T_s	Torque exerted on the sun gear

應用基本路徑圖於具有無段變速器的

複合動力系統之設計

郭先予　劉霆
國立台灣大學機械工程學系

摘 要

本研究提出基本路徑圖(Basic Path Graph, BPG)做為傳動系統拓樸構造的表示方式，並用於設計具有無段變速器(Continuously variable unit, CVU)的複合動力系統。首先介紹其構成元件與所代表的機械構造。接著說明複合動力系統的分類方式，以及所依據的三項特徵：流經 CVU 的動力流方向、動力源間的耦合方式、以及平行於 CVU 的傳動路徑數量。依流經 CVU 的動力流方向，可將系統區分為單向操作與雙向操作兩種；依動力源間的耦合方式，可將系統分為扭力耦合與轉速耦合兩種；而依平行於 CVU 的傳動路徑數量則可將系統區分為單路徑、旁通型雙路徑、與分流型雙路徑三種。其中具有雙向操作特性的系統可擴大系統的速比變化範圍、而分流型雙路徑系統則有助於提升 CVU 的扭力傳輸容量。在欲合成一新系統時，使用 Y 形路徑、單Δ形路徑、與雙Δ形路徑做為骨架，加入對應的元件或拓樸構造，產生其基本路徑圖。應用此方式所產生的可能架構數量，能夠以排列組合公式簡單計算。接著說明將系統發展為完整的機械結構時，構造中必須存在的機構元件與其位置，以確保系統的可行性。最後選擇一具有雙向操作特性、與分流型雙路徑傳動特性的系統做為設計範例，以產生一變速範圍更大、且扭力傳輸容量更高的系統。根據分析結果，此系統能將 CVU 的速比變化範圍擴大 2.7 倍，同時其 CVU 僅傳輸 74%至 92%的輸入扭力與功率。因此使用基本路徑圖所設計的系統，確實具有所要求的特性。